

In Situ ^{13}C MAS NMR Study of *n*-Hexane Conversion on Pt and Pd Supported on Basic Materials

II. On the Mechanism of Isomerization and Hydrocracking

Irina I. Ivanova,^{*,1} Michaël Seirvert,^{*} Anne Pasau-Claerbout,^{*} Niels Blom,[†] and Eric G. Derouane^{*,2}

^{*}Laboratoire de Catalyse, Facultés Universitaires N.-D. de la Paix, 61 Rue de Bruxelles, B-5000 Namur, Belgium; and [†]Haldor Topsøe A/S Research Laboratories, Nymøllevej 55, P.O. Box 213, DK-2800 Lyngby, Denmark

Received January 3, 1996; revised June 21, 1996; accepted July 29, 1996

^{13}C MAS NMR spectroscopy was performed *in situ* to investigate the mechanisms of *n*-hexane isomerization and hydrocracking on Pt and Pd supported on Al-stabilized magnesia (Pt/Mg(Al)O and Pd/Mg(Al)O), and Pt on KL zeolite (Pt/KL). All the catalysts had high metal dispersion, the metal particle sizes being 13, 11, and 18 Å, respectively. *n*-Hexane 1- ^{13}C was used for *in situ* label tracer experiments. ^{13}C MAS NMR spectra were obtained during the time course of the reaction at 573 and 653 K. The NMR results were then quantified, and the reaction kinetics were studied. Identification of the primary and secondary labeled reaction products led to the conclusion that both cyclic and bond-shift isomerization mechanisms operate on the three catalysts. In the case of Pt/Mg(Al)O, the cyclic mechanism accounts for 80% of the isomerization products. In the case of Pt/KL and Pd/Mg(Al)O, the contribution of bond-shift reactions increases due to restricted formation of the methylcyclopentane intermediate on the former and to suppressed hydrogenolysis of methylcyclopentane on the latter. A nonselective cyclic isomerization mechanism operates on magnesia catalysts, while on Pt/KL selective bissecondary bond rupturing occurs. Mechanistic pathways of bond-shift and hydrocracking reactions involve both 1,3- and 2,4-metallocyclobutane intermediates in the case of magnesia-supported catalysts, while in the case of the Pt/KL catalyst a 1,3-metallocyclobutane intermediate is preferentially formed. Only terminal scission occurs on Pt/KL. The Pd catalyst demonstrates enhanced activity in demethylation. The observed differences in the mechanistic pathways are explained on the basis of the specific properties of the metal and support. © 1996 Academic Press, Inc.

INTRODUCTION

Monofunctional mechanisms of skeletal rearrangements of hydrocarbons on platinum films, single-crystal surfaces,

¹ Permanent address: Laboratory of Kinetics and Catalysis, Chemical Department, Moscow State University, Vorob'evy vgor, 117234 Moscow, Russia.

² Present address: Department of Chemistry, University of Liverpool, P.O. Box 147, Liverpool L69 3BX, U.K.

and Pt/alumina and Pt/silica catalysts have been studied in detail (1–15) and reviewed several times (16–18).

Isomerization reactions of alkanes are classified as cyclic and bond-shift-type reactions. Two types of cyclic mechanism have been characterized. The “nonselective” cyclic (NSC) mechanism involves 1,5 dehydrocyclization via dicarbene species with two carbon atoms attached to a single metal atom, followed by statistical rupture of all five cyclic C–C bonds and desorption of isomeric products (1–3, 7, 8). In the “selective” cyclic mechanism (SC), 1–5 ring closure occurs via 1–5 dicarbyne and cyclic 1,2 dicarbene intermediates which for obvious geometrical reasons are necessarily attached to two metal atoms. This mechanism accounts for the selective secondary–secondary cyclic C–C bond rupture (4, 5, 7, 8).

The mechanisms proposed for bond-shift isomerization may be divided into three groups depending on the type of precursor species formed on metal surface. The first group of mechanisms (BSh-I) involves, as a precursor, α,α,γ -triadsorbed species proposed by Anderson and Avery (9). This species may further rearrange via two different transition states, either a π -complex of the Dewar type (BSh-Ia) (9), or adsorbed cyclopropane (BSh-Ib), suggested later by Muller and Gault (10). The second mechanism (BSh-II) proposed by McKerverey *et al.* (11) assumes a σ -alkyl adsorbed precursor and transient species which involve a three-center orbital as in nonclassical carbonium ions. The third group of mechanisms (BSh-III) involves a metallocyclobutane precursor suggested by Garin and Gault (5). The transition states include either the carbenoid species (BSh-IIIa) (5) or the nonclassical carbonium-ion-like transient species (BSh-IIIb) (16) derived from the earlier mechanism of McKerverey *et al.* (Bsh-II).

Bond-shift mechanisms can often account not only for isomerization but also for hydrocracking reactions. Hydrocracking or isomerization occur, depending on whether two organic moieties, formed upon C–C bond scission of the precursor, are desorbed or react again.

The predominant mechanism of isomerization or hydrocracking depends on the structure of the reactant (16–18) and the electronic and geometrical properties of a metallic active ensemble (type of metal, crystallographic face, and particle size) (2–8, 12–15, 18–20). Although mechanisms of skeletal rearrangements of hydrocarbons over noble metal supported on nonacidic materials were claimed to be monofunctional and dependent only on the metal component, there are indications of the influence of the support geometry (21–24) and electronic properties (25–40) on the catalyst activity and selectivity. These effects are more significant in the case of Pd catalysts (28–34) and for basic supports such as MgO or KL zeolites (21–27, 31–39). Detailed mechanistic information, however, is lacking.

It has been shown that the mechanisms of skeletal rearrangements of hydrocarbons can be best elucidated by the ^{13}C tracer technique (18). In the classical approach, the fate of the ^{13}C label in the course of the reaction is monitored by GC–MS of the exit gas at the outlet of the flow reactor. In our previous contribution (41), we demonstrated that it can also be done *in situ* using a controlled-atmosphere ^{13}C MAS NMR technique. The main advantage of the latter technique with respect to the former is the ability to monitor the reaction directly on the catalyst and, therefore, to observe different kinds of adsorbed species, to infer their chemical state and mobility, and to identify reaction intermediates and surface active sites (41–47). However, the application of *in situ* ^{13}C MAS NMR technique has several limitations, especially for the reactions leading to an increase of the total pressure in the system, as has been discussed in Part I (41).

In this paper, we aim to clarify the mechanisms of *n*-hexane isomerization and hydrocracking over Pt supported on KL zeolite (Pt/KL), and Pt and Pd supported on aluminum-stabilized magnesium oxide (Pt/Mg(Al)O and Pd/Mg(Al)O, respectively), and to infer the influence of the metal component and the basic support on these mechanisms by means of *in situ* ^{13}C MAS NMR tracer technique. The identification of the reaction products and intermediates made in Part I (41) is the basis for this study.

EXPERIMENTAL

Materials

Reactants. *n*-Hexane $1\text{-}^{13}\text{C}$ (99.9% enriched) used as labeled reactant was obtained from ICON Services Inc. Methylcyclopentane was obtained from Aldrich Chemical Company.

Catalysts. Pt supported on KL zeolite (Pt/KL), Pt supported on Al-stabilized MgO (Pt/Mg(Al)O), and Pd supported on Al-stabilized MgO (Pd/Mg(Al)O) catalysts were prepared by impregnation as described in Part I (41). The calcined materials were reduced prior to catalytic tests in a flow of H_2 at 700 K for 2 h.

The final metal loadings determined by ICP emission analysis were 1.85 wt% for Pt/KL, 1.12 wt% for Pt/Mg(Al)O and 0.78 wt% for Pd/Mg(Al)O. The metal dispersions determined from isotherms of dihydrogen adsorption [41] were 0.63, 0.89, and 0.93, respectively, and the sizes of metal particles calculated from dispersions were consequently 18, 13, and 11 Å, respectively.

In Situ ^{13}C MAS NMR Measurements

In situ MAS NMR measurements were carried out on an MSL-400 Bruker spectrometer operating at 100.6 MHz. The spinning rate was 3.8 kHz. Quantitative conditions were achieved using high-power gated proton-decoupling with suppressed NOE effect ($5\ \mu\text{s}$ 90° pulses; recycling delay is 4 s).

The NMR cells were prepared by flame sealing of the NMR tubes containing activated catalyst and reactant. The detailed procedure is described in Part I (41). The resultant sample cells contained 150 mg of catalyst and 4 mg of reactant.

The *n*-hexane $1\text{-}^{13}\text{C}$ and methylcyclopentane conversions were studied at two temperatures (573 and 653 K). The reactions were carried out by heating the corresponding NMR cells outside the spectrometer. The MAS NMR measurements were performed at 293 K after quenching the sample cells. In a typical experiment the sample cell was first heated for a short duration of time (1–5 min). After collection of the NMR data, it was returned to the reaction conditions and heated for progressively longer periods of time. ^{13}C spectra were thus recorded over the time course of the reaction.

Definitions

Quantification of the NMR results requires a number of definitions which are listed below:

Conversion of the reactant *r* at time *t* ($X_{r,t}$):

$$X_{r,t} = (1 - I_{r,t}/I_{r,0}) \times 100 [\%],$$

where $I_{r,t}$ corresponds to the integral intensity of the reactant *r* NMR resonance after heating the sample cell for *t* min; $I_{r,0}$ corresponds to the integral intensity of the reactant *r* NMR resonance in the initial NMR spectrum.

Yield of reaction product *p* at time *t* ($Y_{p,t}$):

$$Y_{p,t} = I_{p,t}/I_{r,0} \times 100 [\%]$$

where $I_{p,t}$ corresponds to the integral intensity of the product *p* resonance after heating the sample cell for *t* min.

Selectivity to product *p* at time *t* ($S_{p,t}$):

$$S_{p,t} = Y_{p,t}/X_{p,t} \times 100 = I_{p,t}/(I_{r,0} - I_{r,t}) \times 100 [\%].$$

Initial selectivity to product *p* was determined from the initial slope of $Y_{p,t}(X_{p,t})$ plots extrapolated to zero conversion.

RESULTS AND DISCUSSION

In Part I of this series (41), the *in situ* NMR study of *n*-hexane conversion was carried out as a function of temperature. The main reaction products and reaction pathways in NMR/batch conditions were identified and compared with continuous flow microreactor tests. It has been demonstrated that *n*-hexane isomerization in batch conditions begins at 573 K, while for aromatization and cracking the higher temperature of 653 K is required.

To account further for the mechanisms of various reaction pathways a kinetic study was performed. Two sets of experiments at 573 and 653 K, respectively, were carried out as described in the Experimental section. Figures 1–3 show the aliphatic regions of the ^{13}C MAS NMR spectra observed

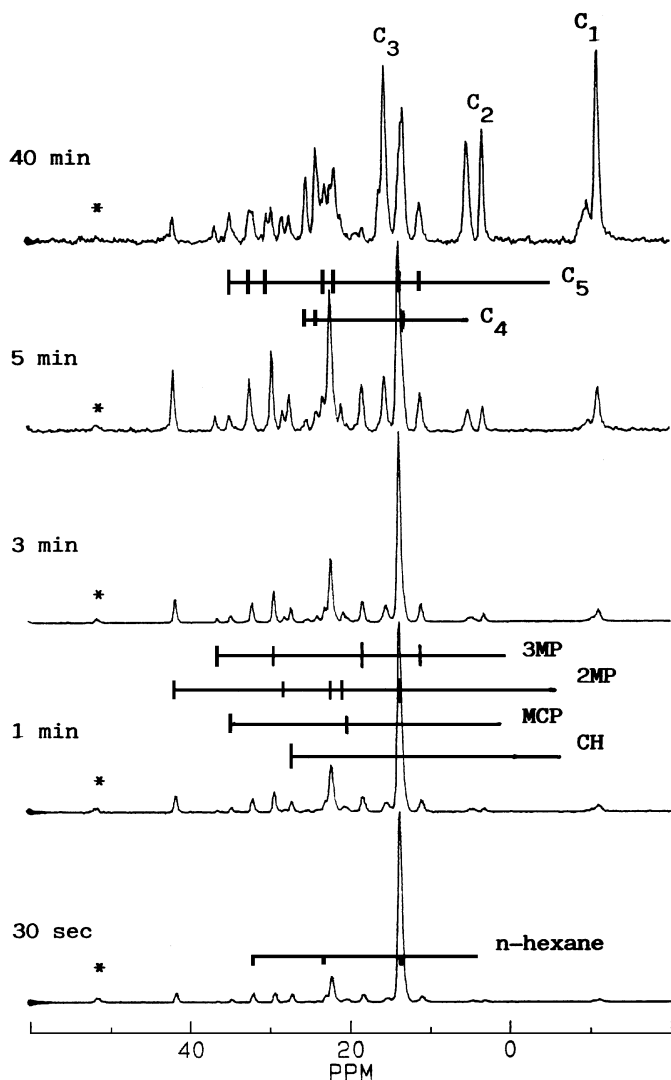


FIG. 1. Aliphatic regions of the ^{13}C MAS NMR spectra observed as a function of reaction time in the course of *n*-hexane $1\text{-}^{13}\text{C}$ reaction at 653 K over Pt/Mg(Al)O catalyst. Asterisk (*) denotes spinning sidebands.

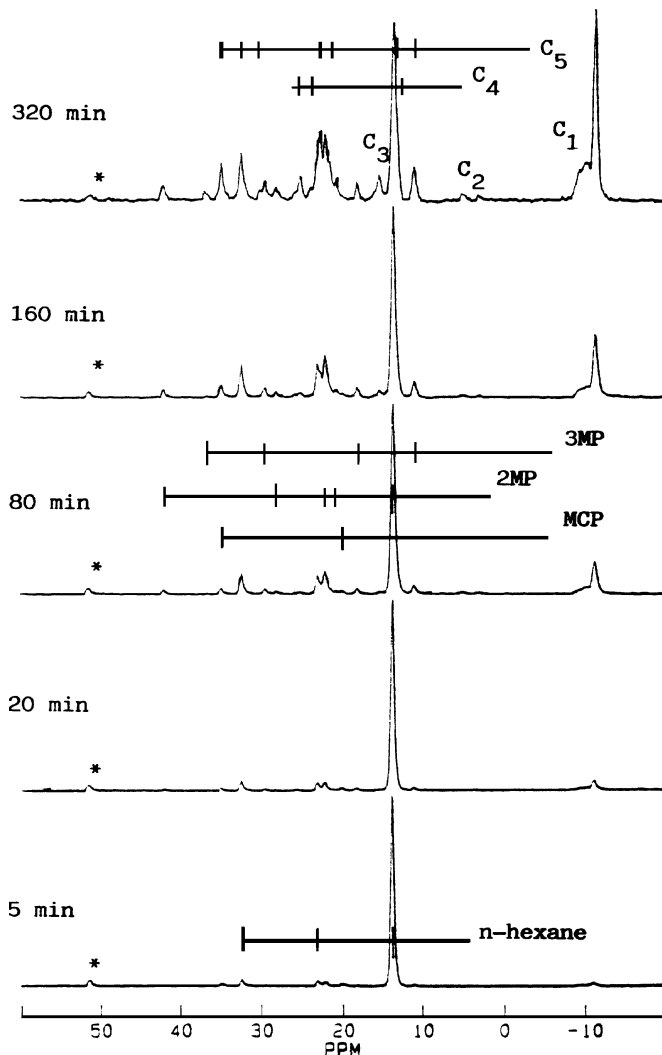


FIG. 2. Aliphatic regions of the ^{13}C MAS NMR spectra observed as a function of reaction time in the course of *n*-hexane $1\text{-}^{13}\text{C}$ reaction at 653 K over Pd/Mg(Al)O catalyst. Asterisk (*) denotes spinning sidebands.

after reaction of *n*-hexane $1\text{-}^{13}\text{C}$ over Pt/Mg(Al)O, Pt/KL and Pd/Mg(Al)O catalysts at 653 K as a function of reaction time. Table 1 lists the observed resonances, their assignments, and the corresponding chemical shifts (referred to TMS) in the gaseous state and in solution. A more detailed description of the line assignments is given in Part I (41).

Isomerization

The main isomerization products observed at 573 K are 2-methylpentane (2MP) and 3-methylpentane (3MP). On Pt/Mg(Al)O, the isomerization is fast. After 40 min of reaction, up to 50% of *n*-hexane is converted to methylpentanes. ^{13}C label scrambling is observed on all the carbon atoms of the methylpentanes. In contrast, on Pt/KL and Pd/Mg(Al)O, the reaction is slow (after 40 min of reaction the conversion is 10 and 2%, respectively).

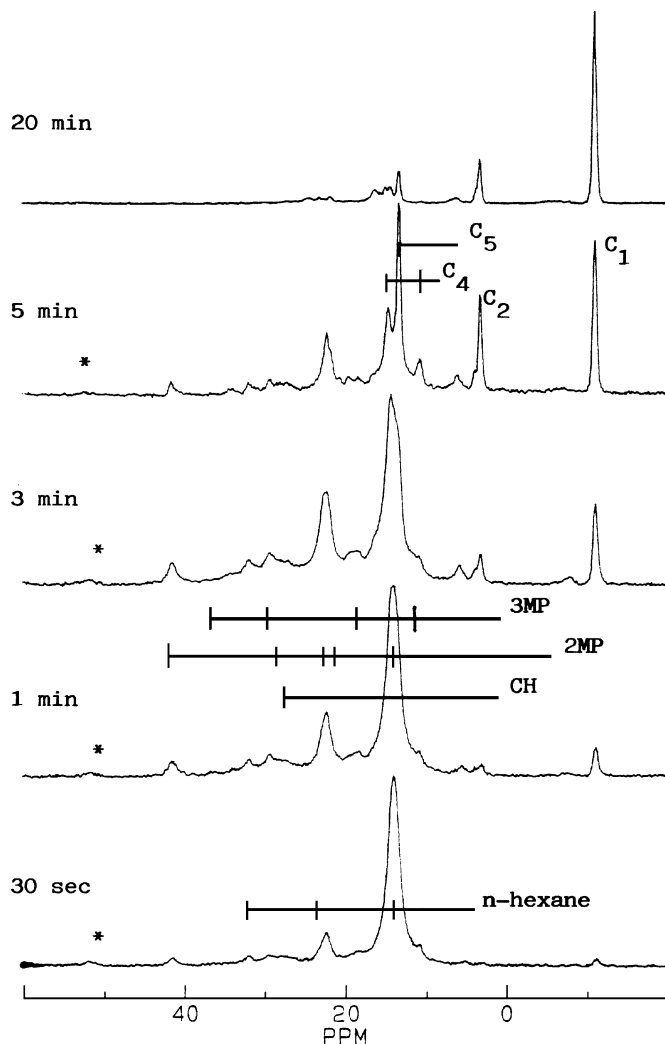


FIG. 3. Aliphatic regions of the ^{13}C MAS NMR spectra observed as a function of reaction time in the course of n -hexane $1\text{-}^{13}\text{C}$ reaction at 653 K over Pt/KL catalyst. Asterisk (*) denotes spinning sidebands.

2-Methylpentane and 3-methylpentane are preferentially labeled on methyl groups.

At 653 K the situation is however different: the reaction is much faster and ^{13}C label scrambling in methylpentanes is observed for all catalysts (Figs. 1–3). Small amounts of 2,3-methylpentane are additionally formed on Pt-catalysts.

By tracing the displacements of the n -hexane $1\text{-}^{13}\text{C}$ carbon atom during the isomerization process and identification of the primary and the secondary labeled products a rough classification of the reactions into two groups (bond-shift and cyclic type) can be made.

Identification of primary and secondary labeled products of isomerization. The identification of the primary and the secondary labeled reaction products was performed using an approach similar to that suggested by Ko and Wojciechowski (48) and applied recently for NMR tracer experiments (49). According to this approach, yields of

labeled reaction products are plotted against conversion. These plots (selectivity patterns) can be used to distinguish between primary (1) and secondary (2), intermediate (I), and final (F) products. The theoretical selectivity patterns characteristic for various types of reaction products are presented in Fig. 4.

To obtain experimental selectivity patterns the NMR line intensities were determined and n -hexane conversions and product yields were calculated as defined in the Experimental section. Yields of differently labeled isomerization products were then plotted versus n -hexane conversion. The products with the selectivity plots of the same type were grouped to simplify the graphs. The experimental selectivity patterns obtained for different groups of isomerization products observed at 653 K on Pt/Mg(Al)O, Pt/KL, and Pd/Mg(Al)O catalysts can be compared with the theoretical ones in Figs. 4 and 5. The selectivity plots for methylcyclopentane are also included, since the latter plays the role of intermediate in cyclic isomerization. Four groups of products are distinguished:

(i) Methylcyclopentane $2\text{-}^{13}\text{C}$ and methylcyclopentane methyl- ^{13}C (group A) are characterized by nonzero slopes on the selectivity plots at zero conversions and by the maximum at rather low conversions. They are identified as primary intermediate products.

(ii) 2-Methylpentane $1\text{-}^{13}\text{C}$ and 3-methylpentane $1\text{-}^{13}\text{C}$ (group B) are also identified as primary intermediate products; however, they show a maximum at higher conversions than methylcyclopentanes. Consequently, the products corresponding to groups A and B are intermediates in different pathways.

(iii) 2-Methylpentane $3\text{-}^{13}\text{C}$, 3-methylpentane $2\text{-}^{13}\text{C}$, and 3-methylpentane methyl- ^{13}C (group C) are characterized

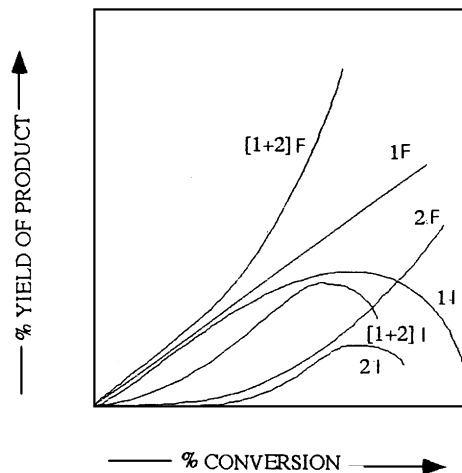
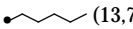
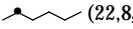

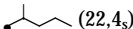
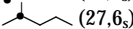
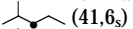
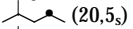
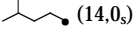

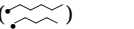
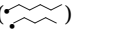
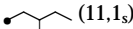
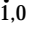
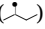
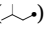
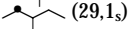
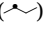
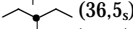
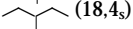
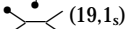
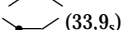
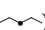
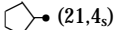
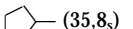
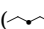

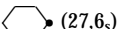
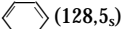
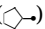

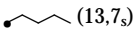
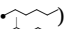
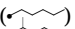
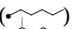
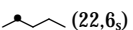
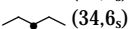
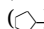
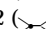
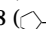
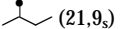
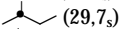
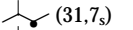
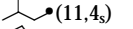
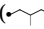
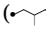
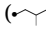
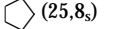
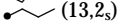
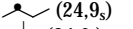
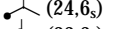
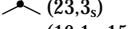
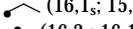
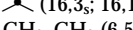


FIG. 4. Theoretical selectivity patterns (48) for intermediate primary (1I), intermediate primary plus secondary ([1+2]I), intermediate secondary (2I), final primary (1F), final primary plus secondary ([1+2]F), and final secondary (2F) products.

TABLE 1
Assignments of the Resonances Observed after Conversion of *n*-Hexane 1-¹³C over Pt/Mg(Al)O, Pt/KL, and Pd/Mg(Al)O Catalysts

| Assignment ^a | Experimental δ (ppm) ^b | | |
|--|--|--|--|
| | Pt/Mg(Al)O | Pt/KL | Pd/Mg(Al)O |
| Reactants | | | |
|  (13,7 _s) | 13,8 | 14,1 | 13,8 |
|  (22,8 _s) | 23,2 | 23,0 | 23,3 |
|  (31,9 _s) | 32,3 | 32,1 | 32,4 |
| Nonidentified | — | 11,0 | — |
| Isomerization products | | | |
|  (22,4 _s) | 22,2 | 22,4 | 22,3 |
|  (27,6 _s) | 28,3 | 28,2 | 28,2 |
|  (41,6 _s) | 41,8 | 41,7 | 41,9 |
|  (20,5 _s) | 21,0 | 20,8 | 20,9 |
|  (14,0 _s) | 13,8 () | 14,1 () | 13,8 () |
|  (11,1 _s) | 11,0 () | 11,0 () | 11,1 () |
|  (29,1 _s) | 29,5 | 29,8 () | 29,5 |
|  (36,5 _s) | 36,7 | — | 36,8 |
|  (18,4 _s) | 18,4 | 18,5 | 18,3 |
|  (19,1 _s) | 19,1 | 19,3 | — |
|  (33,9 _s) | 34,1 | 34,2 () | — |
| Dehydrocyclization products | | | |
|  (21,4 _s) | 20,3 | — | 20,3 |
|  (35,8 _s) | 34,9 () | — | 34,9 () |
|  (27,6 _s) | 27,4 | 27,2 | — |
| Aromatization products | | | |
|  (128,5 _s) | 130,3 | 110–135 | 129,7 |
| Alkylsubstituted benzenes: | | | |
| Methyl (15–21)s | — | — | 20,4 () |
| Ethyl (25–30; 15–16)s | — | — | 28,2 () |
| Aromatic carbons (144–125)s | — | — | 125, 139 |
| Cracking products : | | | |
|  (13,7 _s) | 13,8 () | 14,1 () | 13,8 () |
|  (22,6 _s) | 22,7 | 22,6 | 22,8 |
|  (34,6 _s) | 34,8 () | 34,2 () | 34,8 () |
|  (21,9 _s) | 21,7 | 21,8 | 21,7 |
|  (29,7 _s) | 30,2 | 29,7 | — |
|  (31,7 _s) | 31,9 | 31,5 | — |
|  (11,4 _s) | 11,0 () | 11,0 () | 11,1 () |
|  (25,8 _s) | — | — | 26,0 |
|  (13,2 _s) | 13,2 | 13,3 | 13,3 |
|  (24,9 _s) | 25,3 | 24,8 | 25,3 |
|  (24,6 _s) | 24,3 | 24,1 | 24,1 |
|  (23,3 _s) | 23,9 | 23,4 | 24,0 |
|  (16,1 _s ; 15,4 _g) | 15,6 | 15,0 | 15,5 |
|  (16,3 _s ; 16,1 _g) | 16,2 | 16,5 | 16,1 |
| CH ₃ -CH ₃ (6,5 _s ; 3,2 _g) | 3,2 ; 5,1 | 3,2 ; 5,1 | 3,2; 5,2 |
| CH ₄ (-2,3 _s ; -11 _g) | -11,0 ; -9,7 | -10,9; -5,5 | -11,0; -10,1; -9,8; -9,1 |

Note. (●) indicates ¹³C-labeled carbon atoms.

^a Chemical shifts reported in the literature are given in parentheses: (s) solution data (63); (g) gaseous phase data (64).

^b Other assignments of the corresponding lines are given in brackets.

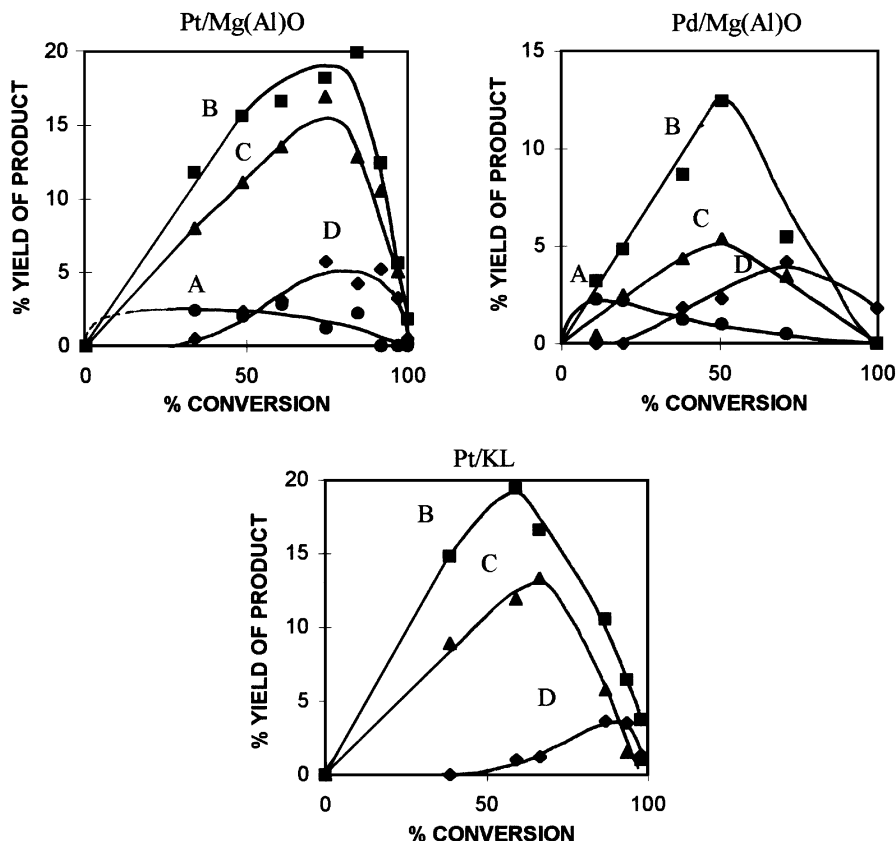


FIG. 5. Experimental selectivity patterns observed for the products of isomerization in the course of *n*-hexane 1-¹³C conversion at 653 K over Pt/Mg(Al)O, Pd/Mg(Al)O, and Pt/KL: (A) Methylcyclopentane 2-¹³C and methylcyclopentane methyl-¹³C. (B) 2-Methylpentane 1-¹³C and 3-methylpentane 1-¹³C. (C) 2-Methylpentane 3-¹³C and 3-methylpentane 2-¹³C and 3-methylpentane methyl-¹³C. (D) 2-Methylpentane 2-¹³C and 2-methylpentane 4-¹³C and 3-methylpentane 3-¹³C.

by zero initial selectivities and therefore are identified as secondary products. They appear at rather low conversions and can arise from methylcyclopentane.

(iv) 2-Methylpentane 2-¹³C, 2-methylpentane 4-¹³C, and 3-methylpentane 3-¹³C (group D) appear at higher conversions, most probably as a result of secondary isomerization of group B and C products.

Labeled methylcyclopentanes were not observed on Pt/KL at 653 K (Fig. 3). However, observation of group C products gives an indication that they are actually formed. This assumption is confirmed by the observation of the traces of methylcyclopentanes at 573 K. Labeled methylcyclopentanes are not detected at 653 K, probably because of their fast conversion into *n*-hexane isomers or because of the overlapping with the nearest signals due to significant line broadening on this catalyst.

The above observations are schematized in Fig. 6. *n*-Hexane 1-¹³C isomerizes via two routes: the first one includes methylcyclopentane as an intermediate and thus represents cyclic type isomerization, the second represents bond shift isomerization. At longer reaction times, the secondary isomerization occurs. All the primary and the sec-

ondary labeled isomerization products possess intermediate behavior due to their cracking at longer contact times (Figs. 1–3).

In conclusion, both cyclic and bond-shift mechanisms are operating on all the catalysts. However, it is evident from Fig. 5 that the contributions of these mechanisms to the overall isomerization depend on the catalyst type.

Contributions of bond-shift and cyclic mechanisms. To evaluate contributions of Cycl and BSh mechanisms on different catalysts the theoretical displacement of the ¹³C label during cyclic and bond-shift isomerization of *n*-hexane 1-¹³C was first considered as shown in Fig. 7. The scheme implies the following primary products of cyclic isomerization: 2-methylpentane 3-¹³C, 3-methylpentane 2-¹³C, 3-methylpentane methyl-¹³C, 2-methylpentane 1-¹³C, *n*-hexane 3-¹³C, and *n*-hexane 1-¹³C. The former three labeled compounds were indeed identified (Figs. 5, 6) as primary labeled products of cyclic isomerization, while NMR resonances corresponding to the latter three compounds may overlap either with bond-shift products or with the resonances from the reactant *n*-hexane, respectively (Table 1).

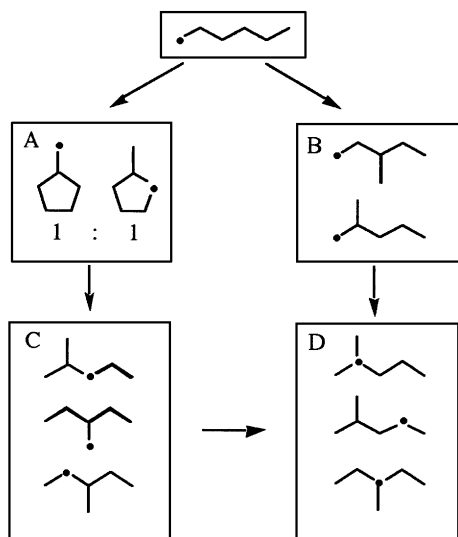


FIG. 6. Primary and secondary products of isomerization observed in the course of *n*-hexane $1\text{-}^{13}\text{C}$ conversion. Reaction network.

Bond shift may occur via methyl shift (MeSH), ethyl shift (EtSH), propyl shift (PrSH) and interconversion (IC). The occurrence of EtSH is evidenced unambiguously by the appearance of 3-methylpentane $1\text{-}^{13}\text{C}$ as a primary reaction product (Figs. 6, 7). Primary formation of 2-methylpentane

$1\text{-}^{13}\text{C}$ suggests the occurrence of MeSH or PrSH (Figs. 6, 7). 2-Methylpentane $5\text{-}^{13}\text{C}$ (another product of MeSH and PrSH) was not identified because of the overlapping with the reactant *n*-hexane $1\text{-}^{13}\text{C}$ (Table 1). The products of interconversion are also overlapping with the reactant.

The next step was to estimate the initial selectivities to the products formed via cyclic and BSh mechanisms. For this, initial selectivities of all the observed nonoverlapping products were first determined as defined in the Experimental section. The results are listed in Table 2. The labeled products were then subdivided into three groups: cyclic only, BSh + cyclic, and BSh only, as shown in Table 2. For the first and the third groups, the initial selectivities via cyclic and BSh routes are equal to the experimental ones (Table 2). For the second group of products, the initial selectivities via different routes were calculated based on theoretical probabilities of the formation of these products relative to the products with known initial selectivity as denoted in footnotes to Table 2. The theoretical probabilities were derived from Fig. 7. It should be mentioned that on the Pt/KL catalyst the resonances corresponding to 2-methylpentane $1\text{-}^{13}\text{C}$ and *n*-hexane $2\text{-}^{13}\text{C}$ overlap (Fig. 3) making impossible the precise calculation of their initial selectivities (Table 2).

The estimated selectivities to cyclic and BSh-type products were further summed up to yield initial selectivities

TABLE 2

Initial Selectivities to Isomerization Products at 653 K

| Products | Pt/Mg(Al)O | | Pd/Mg(Al)O | | | Pt/KL | | | | |
|------------------|----------------|-------------------|------------------|----------------|-------------------|------------------|------------------------|-------------------|--|--|
| | Experimental | Estimated | | Experimental | Estimated | | Experimental | Estimated | | |
| | | Cyclic | BSh | | Cyclic | BSh | | Cyclic | BSh | |
| Cyclic only | | | | | | | | | | |
| | 7.5 | 7.5 | — | 4.0 | 4.0 | — | 5.8 | 5.8 | | |
| | 7.5 | 7.5 | — | 4.0 | 4.0 | — | 5.8 | 5.8 | | |
| | 7.5 | 7.5 | — | 4.0 | 4.0 | — | 5.8 | 5.8 | | |
| | 6.5 | 6.5 | — | 4.5 | 4.5 | — | 2.6 | 2.6 | | |
| Cyclic + BSh | | | | | | | | | | |
| | 26.0 | 25.5 ^a | 3.5 ^b | 18.0 | 12 ^a | 6.0 ^b | (29.4 -) [*] | 17.4 ^a | (12 -) [*] | |
| | Not determined | 19.5 ^c | 5.0 ^d | Not determined | 13.5 ^c | 7.0 ^d | Not determined | 7.8 ^e | (12 - [] _{BSh}) [*] | |
| BSh only | | | | | | | | | | |
| | 5.0 | — | 5.0 | 7.0 | — | 7.0 | (29.4 -) [*] | — | (12 - [] _{BSh}) [*] | |
| | 5.5 | — | 5.5 | 6.0 | — | 8.0 | 3.9 | — | 3.9 | |
| | Not determined | — | 3.5 ^c | Not determined | — | 6.0 ^a | Not determined | — | (12 -) [*] | |
| Selectivity (%) | | 71 | 22.5 | | 42 | 34 | | 45.2 | 27.9 | |
| Contribution (%) | | 76 | 24 | | 57 | 43 | | 62 | 38 | |

Note. (*) - (+) are not resolved.

^a []_C = 3 × [].

^b []_{BSh} = []_{exp} - []_C.

^c []_C = 3 × [].

^d []_{BSh} = [].

^e [] = []_{BSh}.

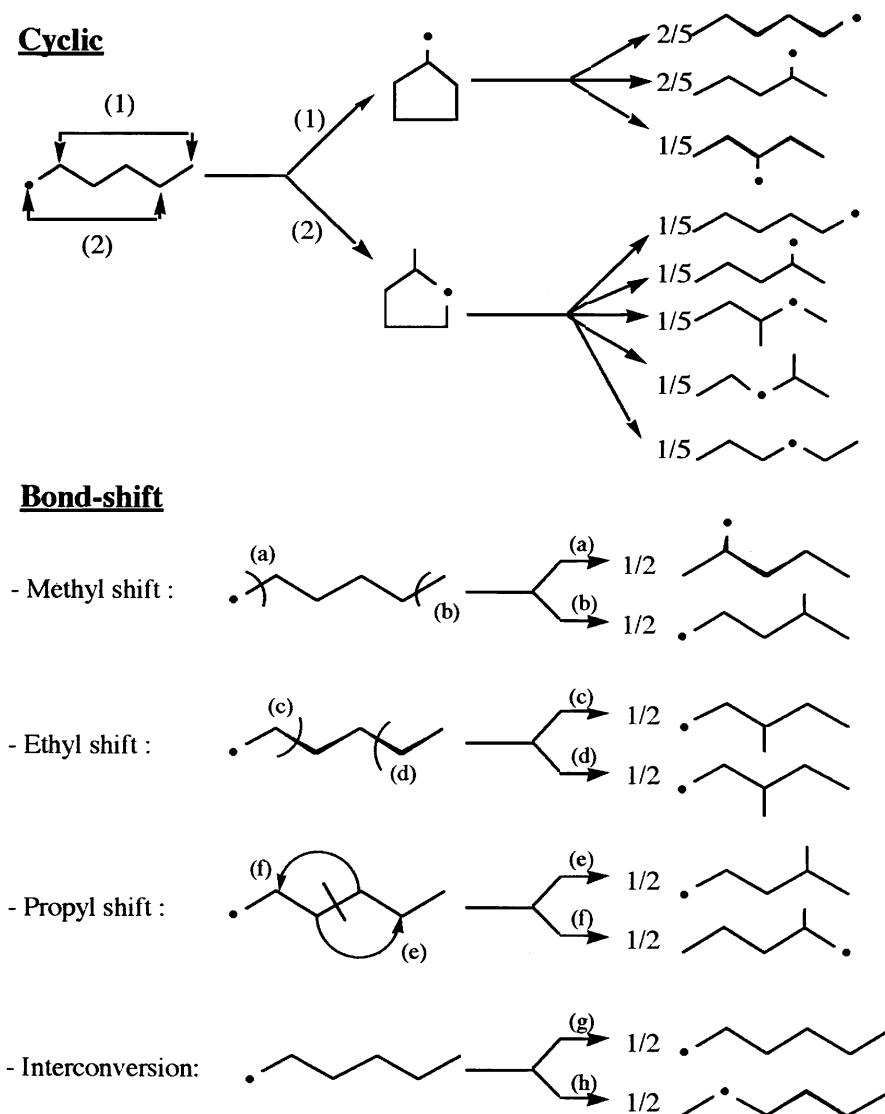


FIG. 7. ^{13}C label displacement during nonselective cyclic and bond-shift isomerization of n -hexane $1\text{-}^{13}\text{C}$.

toward cyclic and BSh isomerization in the overall reaction. Note that the initial selectivities estimated by the above procedure are slightly exaggerated since the products of self-isomerization (n -hexane $1\text{-}^{13}\text{C}$, n -hexane $2\text{-}^{13}\text{C}$, and n -hexane $3\text{-}^{13}\text{C}$) included in total selectivities cannot be taken into account while calculating n -hexane conversion (see Experimental). However, the values of the initial selectivities can be used for the evaluation of the contributions of cyclic and BSh mechanisms to isomerization. Their respective contributions are given in Table 2.

It appears that on Pt/Mg(Al)O catalyst, the isomerization mechanism is predominately cyclic, while on Pd/Mg(Al)O and Pt/KL the contribution of the bond-shift mechanism increases.

Cyclic mechanisms. Cyclic-type isomerization reactions of alkanes were classified as nonselective (NSC) cyclic

and selective cyclic (SC). The NSC mechanism involves statistical rupture of all five cyclic C-C bonds (1-3, 7, 8), while SC mechanism accounts for the selective rupture of the bi-secondary C-C bonds (4, 5, 7, 8).

To determine the probabilities of the rupture of different methylcyclopentane C-C bonds over Pt/Mg(Al)O,

TABLE 3
Probabilities of the Methylcyclopentane Bonds Rupturing during Cyclic Isomerization of n -Hexane $1\text{-}^{13}\text{C}$ at 653 K

| C-C bond | Catalyst | Pt/ Statistical Mg(Al)O | Pd/ Mg(Al)O | Pt/KL | |
|----------|----------|-------------------------------|----------------|-------|-----|
| 1-2 (| | 1 | 1 | 1 | |
| 2-3 (| | 1 | 1.15 | 0.9 | 2.2 |
| 3-4 (| | 1 | 1.15 | 0.9 | 2.2 |

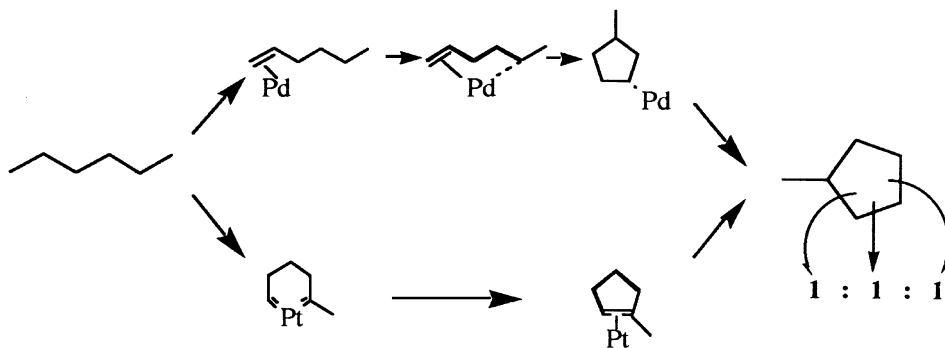


FIG. 8. Mechanism of cyclic isomerization over magnesia-supported catalysts.

Pd/Mg(Al)O, and Pt/KL catalysts the ratios of initial selectivities to *n*-hexane 3-¹³C, 2-methylpentane 3-¹³C, and 3-methylpentane 2-¹³C (or 3-methylpentane methyl-¹³C) were considered, since the formation of these products corresponds unequivocally to rupture of 1-2, 2-3, and 3-4 methylcyclopentane bonds, respectively (Fig. 7). The statistical ratio corresponding to the NSC mechanism is 1:1:1. This distribution is indeed observed on the magnesia-supported catalysts (Table 3), indicating that NSC mechanism operates on both Pt/Mg(Al)O and Pd/Mg(Al)O. Cyclic-type isomerization over Pt/Mg(Al)O most probably occurs via dicarbene species, as a precursor [18] (Fig. 8). This precursor species, however, could hardly be formed on Pd/Mg(Al)O (18, 50). The cyclic mechanism on palladium was proposed to involve, as a precursor, π olefin- σ alkyl 1,2-5 species (18, 31), easily formed on this metal (Fig. 8).

On Pt/KL the situation is different (Table 3). The probability of the rupture of bissecondary C-C bonds is two times higher than that of the secondary-tertiary C-C bond, indicating the replacement of NSC mechanism by SC.

The change from nonselective to selective cyclic mechanism is usually accounted for by decreasing metal dispersion or particle growth. The formation of dicarbene, claimed to be the reactive species in the NSC mechanism, requires only one edge metal atom, while the dicarbene reactive species of the SC mechanism requires two edge atoms. The critical particle size of 20-25 Å, when the NSC mechanism is replaced by SC, corresponds to a cubooctahedron of four atoms on the edge, the smallest structure in which a diadsorbed species involving two contiguous edge atoms may be formed (8, 18).

These considerations, however, cannot be applied in the case of our Pt/KL catalyst, containing Pt particles of 18 Å size, or for the results obtained by Jiang *et al.* on Pt/KL catalysts with very high metal dispersion (51). The cause of a predominant operation of the SC mechanism on this catalyst is still unclear; however, we believe that it is more likely to be due to the geometry of the support (25, 51) than to the specific electronic properties of Pt in zeolite (26).

Bond-shift mechanisms. Formation of 3-methylpentane 1-¹³C, 2-methylpentane 1-¹³C, and *n*-hexane 2-¹³C as primary reaction products suggests that four types of BSH reactions may occur on Pt/Mg(Al)O, Pd/Mg(Al)O, and Pt/KL catalysts (Fig. 7): these are methyl shift (MeSH), ethyl shift (EtSH), propyl shift (PrSH), and interconversion (IC). MeSH and PrSH cannot be distinguished unambiguously because they yield similar labeled products.

The contributions of various pathways to overall isomerization via bond shift were calculated from the initial selectivities to *n*-hexane 2-¹³C and *n*-hexane 1-¹³C (IC), 2-methylpentane 1-¹³C and 2-methylpentane 5-¹³C (MeSH + PrSH), and 3-methylpentane 1-¹³C (EtSH) and are listed in Table 4.

On Pt/Mg(Al)O and Pd/Mg(Al)O, the contributions of various pathways are similar (IC > MeSH + PrSH > EtSH), indicating that the same BSh mechanisms should operate on these catalysts. On Pt/KL, IC, MeSH, and PrSH cannot be distinguished precisely because *n*-hexane 2-¹³C and 2-methylpentane 1-¹³C resonances are not resolved on this catalyst (Tables 2, 4). It is however evident that their contribution increases with respect to EtSH in contrast to magnesia-supported catalysts.

Our experimental observations for the magnesia catalysts are best accounted for by the BSH-IIIa-type mechanism, as shown in Fig. 9. This mechanism involves metallocyclobutane precursors and transition states which consist of carbenoid species. It is assumed that on platinum the metallocyclobutane is formed directly, while in

TABLE 4

Initial Contributions of Alkyl Shifts and Self Isomerization to Bond-Shift Isomerization of *n*-Hexane 1-¹³C at 653 K

| Mechanism | Catalyst Pt/Mg(Al)O | Pd/Mg(Al)O | Pt/KL |
|---------------------|---------------------|------------|-------|
| IC (↔ + ↔) | 44 | 41 | |
| Mesh + PrSh (↔ + ↔) | 31 | 35 | 86 |
| EtSh (↔) | 25 | 24 | 14 |

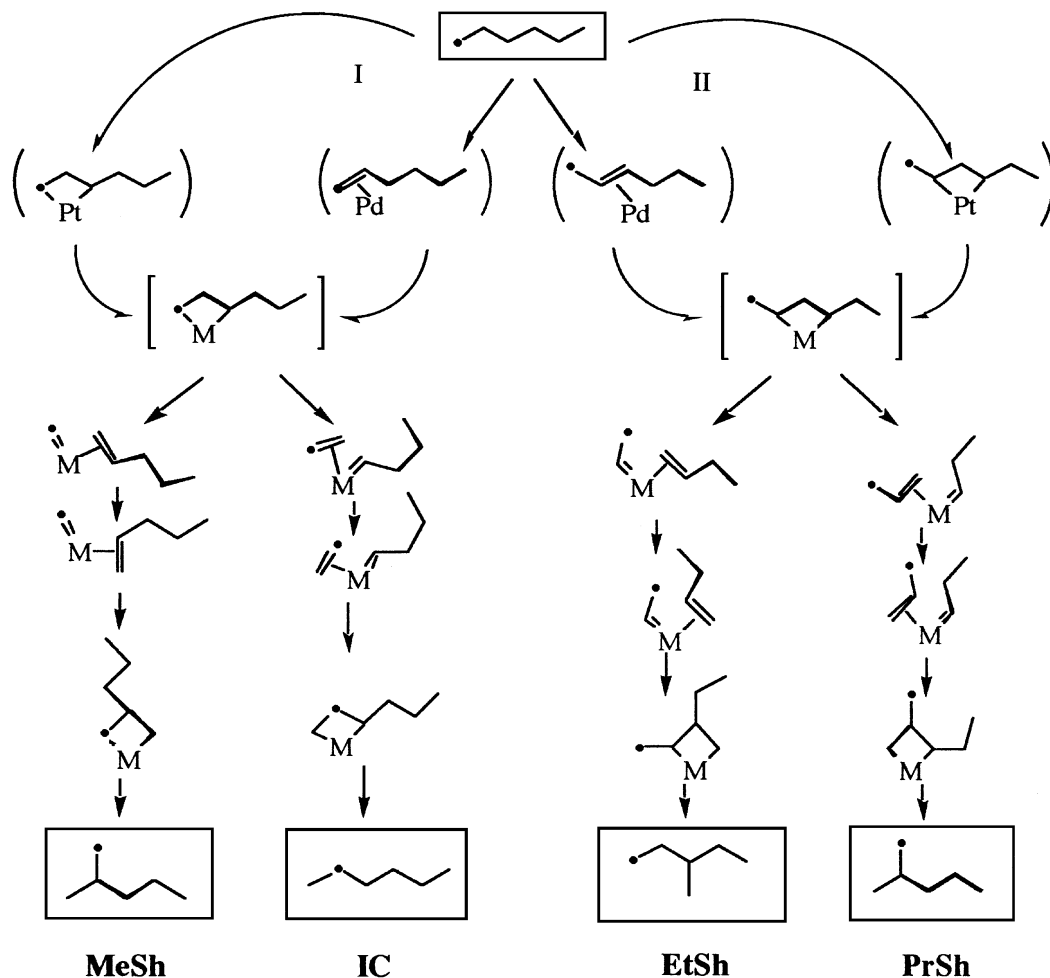


FIG. 9. Mechanism of bond-shift isomerization over magnesia-supported catalysts.

the case of Pd it would result from a transient species of π -olefinic character (18, 31). Two types of metallocyclobutane precursor can be formed from *n*-hexane 1-¹³C, namely, 1,3-metallocyclobutane or 2,4-metallocyclobutane. Each of them can evolve into metallocarbene and π -adsorbed olefin via two different pathways as shown in Fig. 9. Subsequent rotation of π -olefinic species followed by their reaction with metallocarbene, yields the observed isomerization products. 1,3-Metallocyclobutane precursor accounts for IC and MeSH, while 2,4-metallocyclobutane accounts for EtSH and PrSH.

This mechanism easily explains the differences in the rates along various pathways of bond shift isomerization. Indeed, this mechanism assumes the rotation of the adsorbed olefin, a process which requires an activation energy of 10 to 15 kcal/mol (52). The rotation barrier increases by a few kcal if the adsorbed π -olefin is bulky and results in a significant decrease of the corresponding mechanism

contribution. Thus we can explain why IC, which occurs via the smallest π -olefin, has the highest contribution to BSh isomerization. According to this mechanism, isomerization selectivity should decrease in the following order: IC > PrSH > EtSH > MeSH, which is in line with our experimental observations. The formation of 2-methylpentane 1-¹³C and 2-methylpentane 5-¹³C is most probably due to PrSH, while the contribution of MeSH should be the least.

On Pt/KL the formation of 2,4-metallocyclobutane is rather improbable because of the terminal adsorption of *n*-hexane. The unidimensional channel structure of this catalyst will favor the formation of 1,3-metallocyclobutane and preferable realization of the pathway I (Fig. 9) which accounts for IC and MeSH.

In conclusion, both cyclic and bond-shift mechanisms show significant differences on magnesia and zeolite supports.

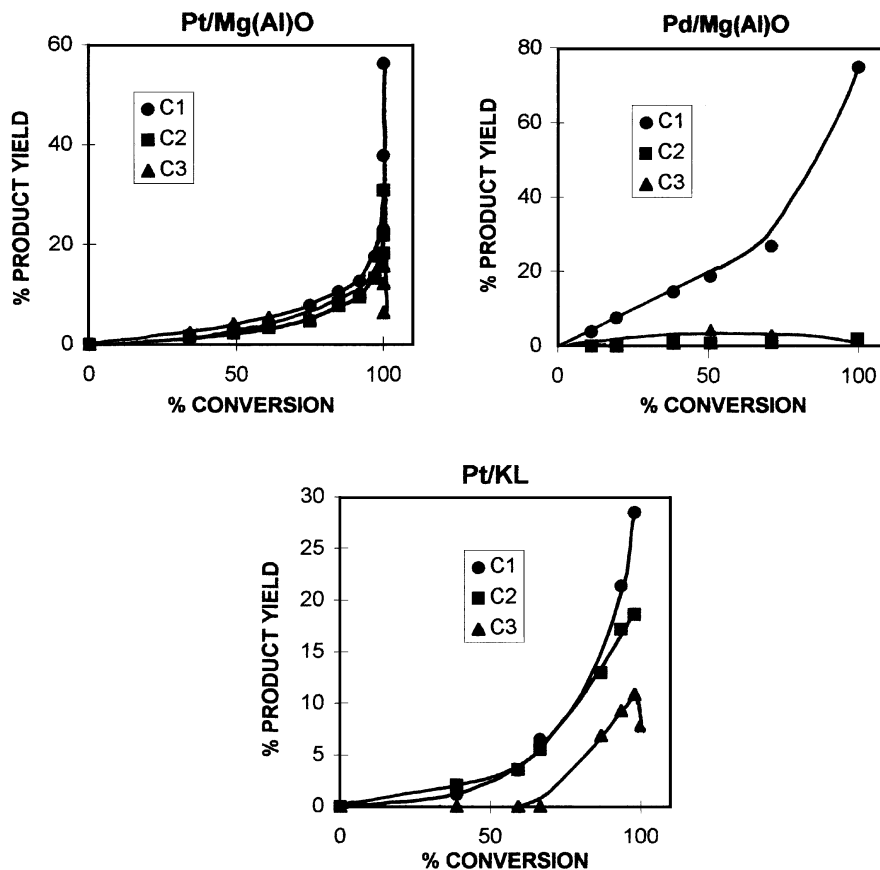


FIG. 10. Experimental selectivity patterns observed for methane (C1), ethane (C2) and propane (C3) in the course of *n*-hexane 1-¹³C conversion at 653 K over Pt/Mg(Al)O, Pd/Mg(Al)O, and Pt/KL.

Hydrocracking

As described in the Experimental part, the conversion of *n*-hexane 1-¹³C was performed in the absence of hydrogen. However, in Part I (41) we demonstrated that no light alkenes but alkanes are formed as a result of *n*-hexane cracking. We thus concluded that cracking reactions performed under our conditions should be referred to as hydrocracking reactions and should be accounted for by hydrogenolysis mechanisms. The source of hydrogen was identified in Part I (41).

Identification of primary and secondary labeled hydrocracking products. The identification of the primary and the secondary labeled hydrocracking products was performed using an approach similar to those previously applied for isomerization.

Yields of methane, ethane, and propane accounting for demethylation (DeMe), deethylation (DeEt), and depropylation (DePr) reactions, respectively, were estimated from the NMR spectra as defined in the Experimental part and plotted versus *n*-hexane conversion. The resultant selectivity patterns observed on Pt/Mg(Al)O, Pt/KL, and Pd/Mg(Al)O catalysts at 653 K (Fig. 10) were compared with the theoretical ones (Fig. 4) and the labeled reaction

products were classified as primary or secondary and intermediate or final. The initial atomic ¹³C selectivities for the primary reaction products were determined from the initial slopes of the selectivity plots. The results are summarized in Table 5.

The hydrocracking products were identified as follows:

(i) Methane is the final reaction product arising from both primary and secondary reactions on all the catalysts. The initial selectivity is an order of magnitude higher on Pd catalyst than on Pt catalysts.

TABLE 5

Identification of the Primary and Secondary Hydrocracking Products and Initial Selectivities

| Product | Catalyst | Pt/Mg(Al)O | Pd/Mg(Al)O | Pt/KL |
|--|----------|------------|------------|---------|
| CH ₄ product type ^a | | (1+2) F | (1+2) F | (1+2) F |
| Initial selectivity | | 5.5 | 38 | 3.1 |
| C ₂ H ₆ product type | | (1+2) F | 1 I | (1+2) F |
| Initial selectivity | | 7.0 | 4.0 | 5.4 |
| C ₃ H ₈ product type | | (1+2) I | 1 I | 2 I |
| Initial selectivity | | 7.2 | 4.0 | 0 |

^a 1, primary; 2, secondary; I, intermediate; F, final.

TABLE 6

Initial Contributions of Hydrocracking Reactions to the Overall Reaction at 653 K

| Reaction | Catalyst | Pt/Mg(Al)O | Pd/Mg(Al)O | Pt/KL |
|----------|----------|------------|------------|-------|
| DeMe | | 34 | 86 | 36 |
| DeEt | | 44 | 9 | 64 |
| DePr | | 22 | 5 | 0 |

(ii) Ethane shows similar behavior to those observed for methane on Pt catalysts. On Pd, it appears as primary intermediate product due to its rapid conversion into methane on this catalyst.

(iii) Propane is an intermediate product on all the catalysts. On Pt/Mg(Al)O, it arises from both primary and secondary reactions. On Pd/Mg(Al)O, it appears only as a primary reaction product, on Pt/KL, only as a secondary one.

In conclusion, different reaction networks are observed on the three catalysts. On Pt/Mg(Al)O, demethylation, deethylation, and depropylation occur simultaneously. At longer reaction times propane is converted to ethane and methane. On Pt/KL, only demethylation and deethylation occur. Propane is formed via secondary reactions; namely demethylation of butane or deethylation of pentane. On Pd/Mg(Al)O, the major primary reaction pathway is demethylation. The initial selectivities of deethylation and depropylation are similar to those observed on Pt/Mg(Al)O. However, on Pd catalyst, propane and ethane are rapidly converted to methane.

Contributions of demethylation, deethylation, and depropylation. The contributions of DeMe, DeEt, and DePr to the overall hydrocracking were calculated from the initial selectivities to these pathways. The initial selectivities to DeMe and DeEt are equal to the respective methane and ethane selectivities. For calculation of the initial selectivity to DePr, the initial selectivity to propane was divided by a factor of two to account for the fact that one hexane molecule gives two propane molecules. The results are summarized in Table 6.

On Pd/Mg(Al)O catalyst, demethylation predominantly occurs. On the contrary, both Pt catalysts favor deethylation: the contribution of depropylation is negligible on Pt/KL catalyst.

The differences in reaction networks and product distribution observed on the three catalysts suggest that different hydrocracking mechanisms are operating.

Hydrocracking mechanisms. Hydrocracking reactions are often accounted for by the bond-shift mechanisms (8, 18). Indeed, the metallocyclobutane mechanism (Fig. 11), similar to those suggested for bond-shift isomerization (Fig. 9), can readily explain the behavior of Pt/Mg(Al)O in hydrocracking reactions. According to this mechanism, the following ratios between

different hydrocracking pathways should be observed: DeMe : DeEt : DePr = 1 : 2 : 1. This is very close to our experimental observations (Table 6). Moreover, this mechanism explains similar initial selectivities to bond-shift isomerization and hydrocracking (Tables 2 and 5). Hydrocracking and bond-shift isomerization are concurrent reaction pathways. They occur, depending on whether the two organic moieties formed upon metallocyclobutane precursor C-C bond scission are desorbed (Fig. 11) or react again (Fig. 9).

Similarly, for Pt/KL, the mechanism suggested for bond-shift isomerization can be extended to hydrocracking reactions. Preferable formation of 1,3-metallocyclobutane as an intermediate on this catalyst results in terminal scission of *n*-hexane and formation of methane and pentane or ethane and butane.

On the contrary, the specific behavior of the Pd catalyst cannot be accounted for by the bond-shift mechanism. High demethylation activity of palladium has been reported for different Pd catalysts (9, 28, 29, 31, 53, 54). The mechanism of demethylation suggested by Gault (18) includes formation of 1,3-diadsorbed species attached to two Pd atoms. This mechanism can explain hydrocracking reactions on Pd films (9) and supported catalysts with low dispersions (31, 54). However, it can hardly be extended to the catalysts with high dispersion (28, 29, this work).

Tolbert *et al.* (55) and Juszczak *et al.* (29) suggested that demethylation proceeds via insertion of Pd between methyl and the other part of the hydrocarbon molecule. This mechanism, however, requires formation of Pdⁿ⁺ species with high Lewis acidity. The formation of such species was proved to be very likely on Pd/Al₂O₃ (29). It is, however, not evident for other catalysts.

Effect of Metal

The comparison of the catalytic behavior of Pt/Mg(Al)O and Pd/Mg(Al)O in *n*-hexane isomerization and hydrocracking shows the following main differences:

(1) The activity of Pt catalyst in isomerization and hydrocracking is much higher than that of Pd (Figs. 1, 2). The same tendency was reported for Pt and Pd on different supports (8, 9, 18, 31, 53, 54) and was attributed to the specific role of the metal. One of the possible explanations is based on the different mechanisms of *n*-hexane activation on Pt and Pd metals. As was firmly established (18, 31), methylcyclopentane and metallocyclobutane precursors of cyclic and bond shift isomerizations are formed directly on Pt catalyst, while in the case of Pd, they result from transient species of π -olefinic character (Figs. 8, 9). The lower activity of Pd catalysts may thus be related to the necessity of this preliminary activation step.

(2) The selectivity to hydrocracking is much higher in the case of Pd (Figs. 1, 2, Table 5) due to the specific ability of this metal to catalyze demethylation.

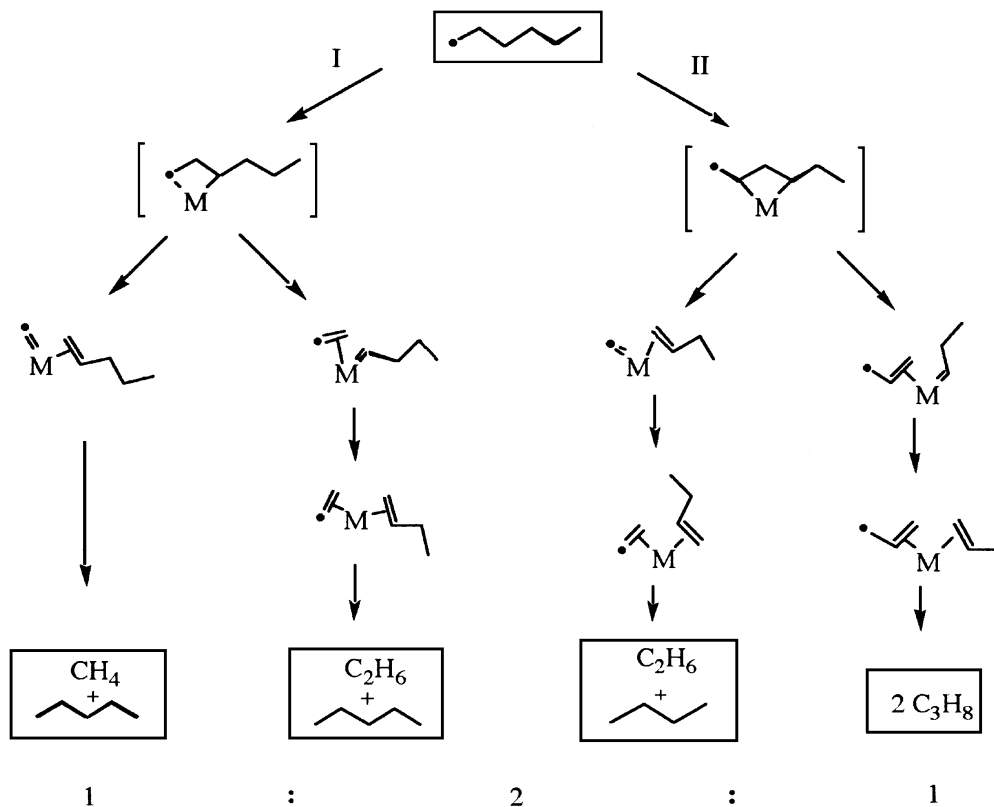
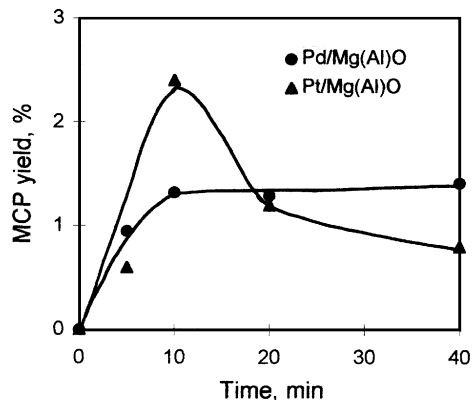


FIG. 11. Mechanism of hydrocracking on Pt/Mg(Al)O.

(3) Cyclic-type isomerization is the major pathway on Pt/Mg(Al)O, while on Pd catalyst the contribution of bond shift reactions increases up to 40% (Table 2). The lower contribution of cyclic isomerization on the less active Pd/Mg(Al)O may be due to the fact that the activation energy of the cyclic isomerization is much higher (50 kJ/mol) than that of the bond shift (56). Another explanation is based on the restricted methylcyclopentane hydrogenolysis on this catalyst. The variation of methylcyclopentane yield with reaction time in the course of *n*-hexane conversion is compared for Pt and Pd in Fig. 12. On Pt catalyst, after the initial increase, the methylcyclopentane concentration immediately decreases due to hydrogenolysis. On the contrary, in the presence of Pd, no conversion of methylcyclopentane, formed during reaction at 573 K, was observed, suggesting that on Pd, methylcyclopentane hydrogenolysis is a limiting step in *n*-hexane cyclic isomerization.

To check this hypothesis the model reaction of methylcyclopentane conversion was carried out at 653 K. The results for Pt/Mg(Al)O and Pd/Mg(Al)O catalysts are compared in Fig. 13. The initial rates of methylcyclopentane hydrogenolysis determined from the initial slopes of kinetic curves for methylcyclopentane are two orders of magnitude lower on Pd than on Pt, while the initial rates of *n*-hexane dehydrocyclization to methylcyclopentane are similar on these catalysts (Fig. 12). This confirms the above assumption.

Similar conclusions were obtained by Kazanskii and Bulanova (57) while studying hydrogenolysis of cyclopentane hydrocarbons over Pd/charcoal. However, the same was not true for Pd/alumina. Gault *et al.* (8) showed that the mechanism of isomerization is predominantly cyclic on Pd/Al₂O₃ independently of metal dispersion. Le Normand *et al.* (31) have found that on Pd/Al₂O₃ the slow step is dehydrocyclization. These discrepancies in the behavior of Pd supported on different materials point to the important

FIG. 12. Variation of methylcyclopentane yield as a function of reaction time in the course of *n*-hexane conversion at 573 K on Pt/Mg(Al)O and Pd/Mg(Al)O catalysts.

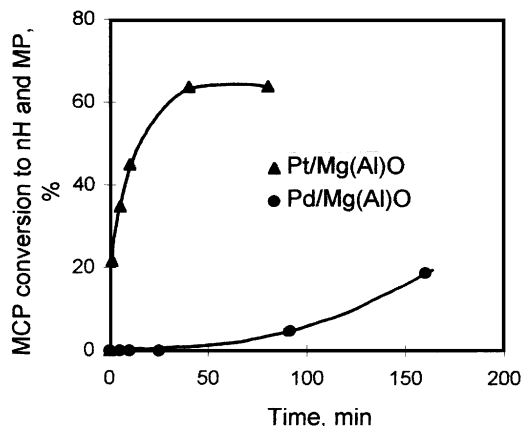


FIG. 13. Methylcyclopentane hydrogenolysis (conversion to *n*-hexane and methylpentanes) as a function of reaction time in the course of methylcyclopentane reaction at 653 K on Pt/Mg(Al)O and Pd/Mg(Al)O catalysts.

role of metal–support interactions for this type of reaction, especially in the case of Pd catalysts.

Effect of Support

The influence of the support on the metal-catalyzed reactions can be classified as geometrical or chemical. Geometrical effects include a support shape selectivity for the diffusion and adsorption of reactants and the formation and diffusion of products and intermediates (21, 23), or nest effects favoring a preorganization of the reactant so as to obtain the intermediate species with an optimal van der Waals interaction with the surface (22). Chemical effects include metal–support interaction and direct participation of the active sites of the support in the reaction. Thus, the bifunctional mechanism was claimed for metals supported on acidic materials (17, 58, 59). In contrast, hydrocarbon conversion on metals supported on neutral and basic materials is generally considered to occur only on the metal component (18, 32, 35, 38). The effect of the support in these cases is due to metal–support interaction (26–40).

Metal–support interaction. Strong metal–support interaction can modify both the electronic and atomic state of the metal in the supported catalyst. It was shown that metal can become electron-deficient (29, 33, 34, 40, 60, 61) or electron-enriched (26, 30, 33, 34, 38) depending on the nature of the support and the type of the catalyst pretreatment. The electron deficiency concept was accepted for Pt and Pd supported on acidic zeolites (40, 60, 61) and Al₂O₃ (25). On the contrary, metals supported on basic forms of zeolites (26, 33, 34) or magnesia (30, 38) were suggested to be electron enriched. The general conclusion emerging from these results is that electron transfer depends on the acid–base properties of the support. Acidic supports attract electrons from the metal, while basic materials favor electron transfer from the support to the metal.

Catalytic consequences of the electron deficiency of the metal are high hydrogenation (40), hydrogenolysis and hydrocracking (29, 33, 34, 55) activities. The electron enrichment of the metal causes the suppression of hydrogen chemisorption (38) and enhances activity in dehydrocyclization (26, 62) and dehydrogenation (62) with respect to hydrogenolysis (38) and hydrogenation (26, 62) reactions.

Our results are in line with this general tendency. The high dehydrogenation and aromatization activities of Pt and Pd supported on magnesia or KL basic materials may be related to a shift of negative charge from the support to the metal.

The discrepancy observed for *n*-hexane dehydrocyclization and methylcyclopentane hydrogenolysis over Pd/Al₂O₃ (31), Pd-charcoal (57), and Pd/Mg(Al)O (this work) may also be explained by the effect of support. Pd on alumina is electron deficient, and thus must favor MCP hydrogenolysis and consequently cyclic type isomerization. On Pd supported on magnesia, MCP hydrogenolysis is prevented and the contribution of bond shift isomerization increases.

Geometrical effects. Geometrical effects of a support on *n*-hexane conversion can be inferred from the comparison of the catalytic properties of Pt/Mg(Al)O and Pt/KL. These catalysts are characterized by the same type of metal with similar dispersion. Both supports have basic properties. The main difference is related to the support geometry. Pt/KL has a unidimensional channel (7 Å) structure collimating the diffusing flux of *n*-hexane molecules so that their long axis is parallel to the zeolite channel (21, 23). Mg(Al)O carrier has no analogous channel system which is able to confine the reactant (32, 35–37).

Catalytic consequences of these differences, observed in *n*-hexane isomerization and hydrocracking can be summarized as shown in Fig. 14.

(1) *n*-hexane adsorption occurs upon methylene groups on the magnesia catalyst, and upon methyl groups on zeolite. The adsorbed species are restricted in mobility within zeolite channels (41).

(2) The contribution of the cyclic mechanism to isomerization is lower on Pt/KL comparatively to Pt/Mg(Al)O, due to less favorable 1–5 ring closure with respect to 1–6 ring closure, induced by zeolite confinements (21–23).

(3) The cyclic-type isomerization mechanism is nonselective on Pt/Mg(Al)O and selective on Pt/KL, because of restricted mobility of methylcyclopentane intermediate within zeolite channels.

(4) The differences in the distribution of labelled products observed for bond shift isomerization over magnesia and zeolite catalysts suggest different mechanisms, including 1,3- and 1,4-metallocyclobutane on Pt/Mg(Al)O and only 1,3-metallocyclobutane on Pt/KL.

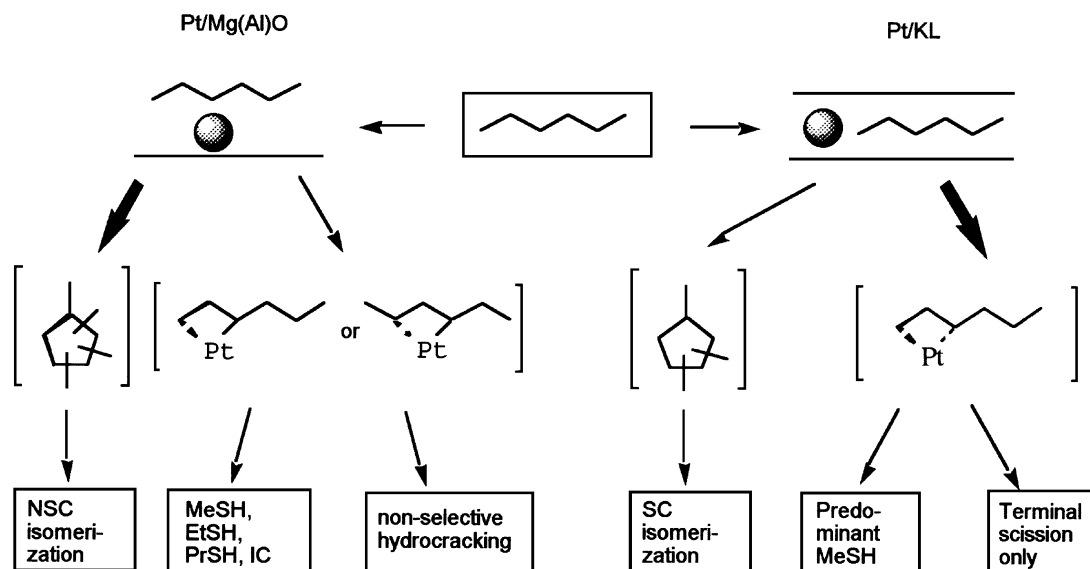


FIG. 14. Effect of the support on the catalytic behavior of platinum in *n*-hexane skeletal rearrangements.

(5) On Pt/Mg(Al)O internal and terminal scissions have equal probabilities, while Pt/KL favors terminal scission due to terminal adsorption.

CONCLUSIONS

(i) Isomerization and hydrocracking of *n*-hexane on Pt/Mg(Al)O was found to obey rules similar to those discovered by Gault and co-workers for Pt/alumina. The non-selective cyclic mechanism accounts for 80% of isomerization products. The metallocyclobutane mechanism explains the behavior of Pt/Mg(Al)O in bond-shift isomerization and hydrocracking.

(ii) The behavior of Pd/Mg(Al)O in isomerization was accounted for by the same mechanisms. However, the activity of this catalyst is found to be much lower. The contribution of bond shift isomerization increases the expense of cyclic isomerization, because hydrogenolysis of methylcyclopentane intermediate becomes a limiting step of cyclic isomerization. The selectivity to hydrocracking is much higher due to the specific ability of this metal to catalyze demethylation. The differences are related to the specific properties of the metal and strong metal-support interaction.

(iii) The unidimensional channel structure of Pt/KL causes terminal adsorption of *n*-hexane and restricted mobility of adsorbed species. The catalytic consequences result in mechanistic pathways different from those suggested for Pt and Pd on Mg(Al)O: selective cyclic isomerization with preferential bisecondary bond rupturing and bond shift isomerization and hydrocracking via preferential formation of 1,3-metallocyclobutane intermediate. The contribution of the cyclic mechanism to isomerization is lower on Pt/KL comparatively to Pt/Mg(Al)O due to less favorable 1–5 ring

closure with respect to 1–6 ring closure, induced by zeolite confinements. Terminal scission is favored because of terminal adsorption.

ACKNOWLEDGMENTS

I. I. Ivanova thanks the Belgian Program on Interuniversity Attraction Poles (PAI), Haldor Topsoe A/S and the Laboratoire de Catalyse (FUNDP) for a research postdoctoral position. The authors thank G. Daelen for technical assistance.

REFERENCES

- Barron, Y., Cornet, D., Maire, G., and Gault, F. G., *J. Catal.* **2**, 152 (1963).
- Barron, Y., Maire, G., Muller, J. M., and Gault, F. G., *J. Catal.* **5**, 428 (1966).
- Corolleur, C., Corolleur, S., and Gault, F. G., *J. Catal.* **24**, 385 (1972).
- Corolleur, C., Tomanova, D., and Gault, F. G., *J. Catal.* **24**, 401 (1972).
- Garin, F., and Gault, F. G., *J. Am. Chem. Soc.* **97**, 4466 (1975).
- Parayre, P., Amir-Ebrahimi, V., and Gault, F. G., *J. Chem. Soc. Faraday Trans. 1* **76**, 1723 (1980).
- Amir-Ebrahimi, V., and Gault, F. G., *J. Chem. Soc. Faraday Trans. 1* **76**, 1735 (1980).
- Gault, F. G., Amir-Ebrahimi, V., Garin, F., Parayre, P., and Weisang, E., *Bull. Soc. Chem. Belg.* **88**, 475 (1979).
- Anderson, J. R., and Avery, N. R., *J. Catal.* **5**, 446 (1966).
- Muller, J. M., and Gault, F. G., in "Symposium on Mechanisms and Kinetics of Complex Catalytic Reactions, Moscow, 1968," Paper 15.
- McKervey, M. A., Rooney, J. J., and Samman, N. G., *J. Catal.* **30**, 330 (1973).
- Garin, F., Aeiayach, S., Légaré, P., and Maire, G., *J. Catal.* **77**, 323 (1982).
- Davis, S. M., Zaera, F., and Somorjai, G. A., *J. Catal.* **85**, 206 (1984).
- Zaera, F., Godbey, D., and Somorjai, G. A., *J. Catal.* **101**, 73 (1986).
- Dauscher, A., Garin, F., and Maire, G., *J. Catal.* **105**, 233 (1987).
- Clarke, J. K. A., and Rooney, J. J., *Adv. Catal.* **25**, 125 (1976).

17. Gates, B. C., Katzer, J. R., and Schuit, G. C. A., "Chemistry of Catalytic Processes," McGraw-Hill, New-York, 1979.
18. Gault, F. G., *Adv. Catal.* **30**, 1 (1981).
19. Primet, M., Basset, J. M., Garbowski, E., and Mathieu, M. V., *J. Am. Chem. Soc.* **97**, 3655 (1975).
20. Takasu, Y., Unwin, R., Tesche, B., and Bradshaw, A. M., *Surf. Sci.* **77**, 219 (1978).
21. Tauster, S. J., and Steger, J. J., *Mater. Res. Soc. Proc.* **111**, 419 (1988).
22. Derouane, E. G., and Vanderveken, D., *Appl. Catal.* **45**, L15 (1988).
23. Tauster, S. J., and Steger, J. J., *J. Catal.* **125**, 387 (1990).
24. Lane, G. S., Modica F. S., and Miller, J. T., *J. Catal.* **129**, 145 (1991).
25. Lerner, B. A., Carvill, B. T., and Sachtler, W. M. H., *J. Mol. Catal.* **77**, 99 (1992).
26. Besoukhanova, C., Guidot, J., Barthomeuf, D., Breyse, M., and Bernard, J. R., *J. Chem. Soc. Faraday Trans. 1* **77**, 1595 (1981).
27. Larsen, G., and Haller, G. L., *Catal. Lett.* **3**, 103 (1989).
28. Juszczuk, W., and Karpinski, Z., *J. Catal.* **117**, 519 (1989).
29. Juszczuk, W., Karpinski, Z., Ratajczykowa, I., Stanasiuk, Z., Zielinski, J., Sheu, L.-L., and Sachtler, W. M. H., *J. Catal.* **120**, 68 (1989).
30. Figueras, F., Gomez, R., and Primet, M., *Adv. Chem. Ser.* **121**, 480 (1973).
31. Le Normand, F., Kili, K., and Schmitt, J. L., *J. Catal.* **139**, 234 (1993).
32. Derouane, E. G., Jullien-Lardot, V., Davis, R. J., Blom, N., and Højlund-Nielsen, P. E., *Stud. Surf. Sci. Catal.* **75**, 1031 (1993).
33. Miller, J. T., Modica, F. S., Meyers, B. L., and Koningsberger, D. C., *Prepr. ACS Div. Petr. Chem.* **38**, 825 (1993).
34. Mojet, B. L., Kappers, M. J., Muijsers J. C., Niemantsverdriet, J. W., Miller, J. T., Modica, F. S., and Koningsberger, D. C., *Stud. Surf. Sci. Catal.* **84**, 909 (1993).
35. Derouane, E. G., Jullien-Lardot, V., Pasau-Claerbout, A., Blom, N. J., and Højlund-Nielsen, P. E., North American Catalysis Meeting (1993).
36. Davis, R. J., and Derouane, E. G., *Nature* **349**, 313 (1991).
37. Davis, R. J., and Derouane, E. G., *J. Catal.* **132**, 269 (1991).
38. Clarke, J. K. A., Bradley, M. J., Garvie, L. A. J., Craven, A. J., and Baird T., *J. Catal.* **143**, 122 (1993).
39. Goldwasser, J., Bolivar, C., Ramon Ruiz, C., Arenas, B., Wanke, S. E., Royo, H., Barrios, R., and Giron, J., in "Proceedings 8th International Congress on Catalysis, Berlin, 1984," Vol. 5, p. 195. Verlag-Chemie, Weinheim, 1984.
40. Schwank, J., Parravano, G., and Gruber, H. L., *J. Catal.* **61**, 19 (1980).
41. Ivanova, I. I., Pasau-Claerbout, Seirvert, M. A., Blom, A., and Derouane, E. G., *J. Catal.* **158**, 521 (1996).
42. Anderson, M. W., and Klinowski, J., *Nature* **339**, 200 (1989).
43. Haw, J. F., Richardson, B. R., Oshiro, I. S., Lazo, N. D., and Speed, J. A., *J. Am. Chem. Soc.* **111**, 2052 (1989).
44. Haw, J. K., *Spec. Publ. - R. Soc. Chem. London* **114**, 1 (1992).
45. Ivanova, I. I., and Derouane, E. G., *Stud. Surf. Sci. Catal.* **85**, 357 (1994).
46. Derouane, E. G., Abdul Hamid, S. B., Ivanova, I. I., Blom, N., and Højlund-Nielsen, P.-E., *J. Mol. Catal.* **86**, 371 (1994).
47. Nowak, A. K., Wilson, A. E., Roberts, K., and Datema, K. P., *J. Catal.* **144**, 495 (1993).
48. Ko, A. N., and Wojciechowski, B. W., *Prog. React. Kinet.* **12**, 201 (1983).
49. Ivanova, I. I., Blom, N., Abdul Hamid, S. B., and Derouane, E. G. *Rec. Trav. Chim. Pays-Bas* **113**, 454 (1994).
50. Muller, J. M., and Gault, F. G., *J. Catal.* **24**, 361 (1972).
51. Jiang, H. J., Tzou, M. S., and Sachtler, W. M. H., *Appl. Catal.* **39**, 255 (1988).
52. Byrne, J. W., Blaser, H. V. and Osborn J. A., *J. Am. Chem. Soc.* **97**, 3871 (1975).
53. Paál, Z., and Tétényi, P., *Appl. Catal.* **1**, 9 (1981).
54. Hajek, M., Corolleur, S., Corolleur, C., Maire, G., O'Kinneide, A., and Gault, F. G., *J. Chem. Phys. - Chem. Biol.* **71**, 1329 (1974).
55. Tolbert, M. A., Mandich, M. L., Halle, L. E. and Beauchamp, J. L., *J. Am. Chem. Soc.* **108**, 5675 (1986).
56. Maire, G., and Garin, F., in "Catalysis: Science and Technology" (J. R. Anderson and M. Boudart, Eds.), Vol. 6, p. 161. Springer-Verlag, Berlin 1984.
57. Kazanskii, B. A., and Bulanova, T. F., *Dokl. Akad. Nauk SSSR Ser. Khim.* **62**, 83 (1948).
58. Ciapetta, F. G., and Wallace D. N., *Catal. Rev.* **5**, 67 (1972).
59. Marin, G. B., and Froment, G. F., *Chem. Eng. Sci.* **37**, 759 (1982).
60. Dalla Betta, R. A., and Boudart, M., in "Proceedings, 5th International Congress on Catalysis, Palm Beach, 1972" (J. W. Hightower, Ed.), Vol. 2, p. 1329. North-Holland, Amsterdam, 1973.
61. Gallezot, P., *Catal. Rev.* **20**, 121 (1979).
62. Bernard, J. R., in "Proceedings, 5th International Zeolite Conference" (L.V. Rees, Ed.), p. 686. Heyden, London, 1980.
63. Breitmaier, E., and Voelter, W., "Carbon-13 NMR Spectroscopy," V.C.H., Weinheim, 1987.
64. Nagy, B., Engelhardt, G., and Michel, D., *Adv. Colloid Interface Sci.* **23**, 67 (1985).